THE JOURNAL OF PHYSICAL CHEMISTRY C
A JOURNAL OF THE AMERICAN CHEMICAL SOCIETY

pubs.acs.org/JPCC

Article

Thin-Film Polyisocyanide-Based Hydrogels for Affinity Biosensors

Daria Kotlarek, Kaizheng Liu, Nestor G. Quilis, Dominik Bernhagen, Peter Timmerman, Paul Kouwer,* and Jakub Dostalek*

Cite This: *J. Phys. Chem. C* 2021, 125, 12960−12967

Read Online

ACCESS | Metrics & More | Article Recommendations | Supporting Information

ABSTRACT: A new type of hydrogel thin film that can be post-modified with biofunctional molecules is investigated for possible applications in evanescent wave optical affinity biosensors. This material is based on a polyisocyanide (PIC) copolymer that self-assembles into a fibrous polymer network. It is covalently tethered to a solid transducer surface, and its swelling gives rise to a hydrogel layer with a thickness up to several micrometers, as characterized by a combination of surface plasmon resonance and optical waveguide spectroscopy. Thin PIC-based hydrogel films with pendant functional biomolecules can be used in label-free affinity sensing strategies. In this work, we demonstrate the PIC-based affinity binding matrix through an avidin coupling of functional biomolecules and immunoassay-based detection, which can be readily expanded to other types of assays and target analytes. In addition, the stable PIC matrix proves to be resistant to fouling, even in the presence of complex biological fluids such as blood plasma or serum.

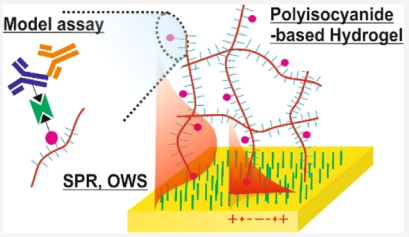

Downloaded via 62.218.164.126 on June 28, 2021 at 15:12:27 (UTC).
See https://pubs.acs.org/sharingguidelines for options on how to legitimately share published articles.

INTRODUCTION

Hydrogels are materials composed of chemically or physically cross-linked polymer chains forming a three-dimensional network that can accommodate large amounts of water. The uptake of water by such a polymer network occurs without dissolving its structure, and it is accompanied by a strong volumetric expansion.[1] On-demand swelling and contraction of such polymer networks can be achieved for a sub-class of (mostly synthetic) responsive hydrogels by applying an external stimulus, for example, temperature,[2] pH,[3] light,[4] pressure,[5] electric, or magnetic fields[6] or through specific interactions with (bio)molecules.[7] Besides, the chemical inertness of many hydrogels endows them with excellent biocompatibility and minimized nonspecific interactions with proteins and cells in complex biological environments. All these features form the basis for widespread hydrogel applications in areas including detection and analysis of chemical and biological species.[8]

Among various bioanalytical tools, evanescent wave optical biosensors, particularly those based on surface plasmon resonance (SPR), have become an established technology for the label-free detection and interaction analysis of (bio)-molecules. The sensing principle is based on probing the sensor surface carrying biorecognition elements for an affinity capture of target species by using a confined electromagnetic field of surface plasmons.[9] Notably, the utilization of a hydrogel-based binding matrix on the surface of SPR-based sensors improves their performance by matching the volume that is optically probed with that where biorecognition elements are immobilized. In this approach, the sensing regime is extended from the conventionally used two-dimensional architectures (e.g., based on self-assembled monolayers) to the three-dimensional systems that allow for the capture of more analyte molecules from the analyzed liquid sample and that provide an environment that better mimics the natural conditions in biomolecular interaction studies.[10,11] Along with these advancements, other modalities of optical transduction were introduced to SPR-based sensors, as the thin hydrogel films at the sensor surface can also act as a dielectric optical waveguide. Optical waveguide spectroscopy (OWS)[12] and fluorescence spectroscopy[13] were employed for optical probing of highly swollen hydrogel films, through which open structure biomolecules can rapidly diffuse and affinity bind. In addition, stimuli-responsive hydrogels were utilized for the actuation of the optical signal in optical affinity SPR-based sensors,[14−16] while their inert chemical nature was exploited for the design of antifouling sensor coatings, enabling the detection of biomarkers in complex biological media.[17−19]

Up to now, hydrogels derived from natural polymers, including polysaccharides and polypeptides (e.g., dextran, cellulose, alginate, chitosan, agarose, collagen, hyaluronic acid, and fibrin), were mostly explored for sensing applications, capitalizing on their porous architectures, nontoxicity, and cost-efficient preparation. However, they typically lack stimulus-responsive characteristics,[20] which limit the implementation of additional functionalities based on the active tuning of their structure. Recently, a new responsive synthetic

Received: March 19, 2021
Revised: May 19, 2021
Published: June 3, 2021

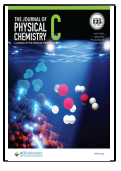

ACS Publications

© 2021 The Authors. Published by American Chemical Society

https://doi.org/10.1021/acs.jpcc.1c02489
J. Phys. Chem. C 2021, 125, 12960−12967

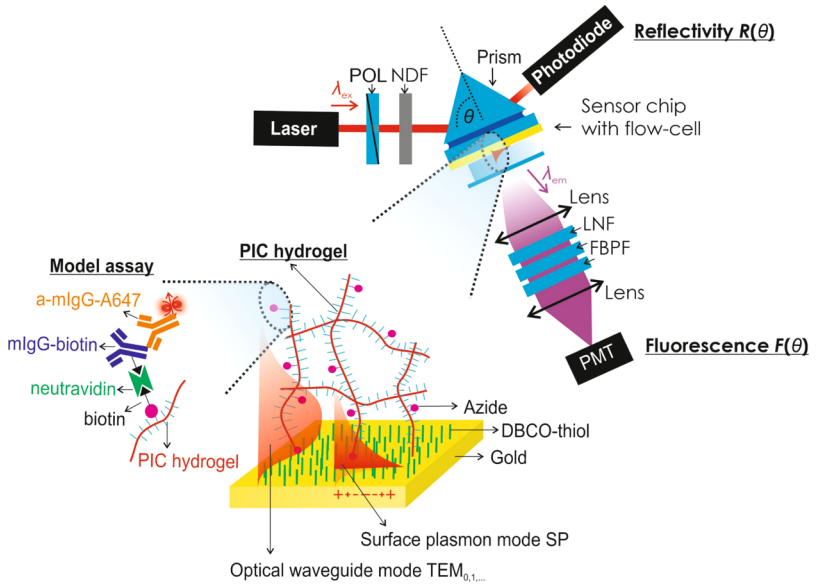

Figure 1. Optical setup employed for the combined SPR, OWS, and fluorescence spectroscopy for the characterization and monitoring of affinity binding events inside the PIC-based thin hydrogel films.

and highly biomimetic gel based on oligo(ethylene glycol)-grafted polyisocyanides (PICs) was developed. The glycol tails introduce a strong thermoresponsive behavior in the material, with a reversible sol−gel transition at $T_{gel} \approx 18$ °C that can be adjusted by the tail length.[21] The helical architecture of PIC is stabilized by the peptidic hydrogen bonds, creating stiff polymer chain bundles providing mechanical strength. Moreover, the polymer can be endowed with additional functional groups for the conjugation with biomolecules (e.g., RGD peptides for enhanced cell adhesion[22]) or cross-linkers. The PIC hydrogel exhibits a stress-stiffening behavior that is widespread in biopolymer matrices, but is, however, rare in synthetic materials. For instance, stress-stiffening of PIC was reported to play an important role in the commitment of stem-cell fate.[23] Due to the biomimetic properties and thermally induced gelation, the PIC hydrogel was used as a bulk material and applied for wound dressing,[22] 3D cell cultures, and tissue engineering[24] and as an injectable scaffold.[25]

In this article, we report on the use of PIC polymers as a matrix for real-time biosensing in complex bioenvironments. Thin hydrogel films were attached to a solid SPR chip through facile PIC click conjugation chemistry and were functionalized with biotin for subsequent biofunctionalization. Swelling of the biomolecule-functionalized PIC hydrogel thin films was observed by OWS combined with SPR. The combination of these evanescent wave techniques with fluorescence spectroscopy was utilized to measure diffusion and affinity binding of biomolecules inside the hydrogel. The possible implementation of this novel material in bioassays and its resistance to fouling from bodily fluids such as blood plasma is demonstrated.

EXPERIMENTAL SECTION

Materials. The dibenzocyclooctyne (DBCO)-PEG4-biotin conjugate was obtained from Sigma-Aldrich (Germany). Neutravidin and rabbit anti-mouse IgG (H + L) antibody conjugated with Alexa Fluor 647 were purchased from Thermo Scientific (Austria). Biotinylated mouse IgG was obtained from Abcam (UK). Phosphate buffer saline tablets (PBS: 140 mM NaCl, 10 mM phosphate, 3 mM KCl, pH = 7.4) were obtained from Calbiochem (Germany). Normal pooled human serum, plasma, and single donor whole human blood were obtained from Innovative Research (USA). All buffer solutions were prepared by using ultrapure water (arium pro, Sartorius Stedim, Germany). Isocyanide monomers were obtained from Chiralix. Absolute ethanol (99.5%) was purchased from Fisher Scientific. Nickel(II)perchlorate hexahydrate was obtained from Sigma-Aldrich.

Synthesis of PIC Copolymers. The PICs were synthesized according to an established protocol.[26] Briefly, the isocyanide monomers (3% carrying an azide group for post-functionalization) were dissolved in freshly distilled toluene, then the catalyst $Ni(ClO_4)_2{\cdot}6H_2O$ (0.1 mg mL^{-1} in freshly distilled toluene/absolute ethanol, 9:1 in volume) was added, and the toluene was added to set the final isocyanide concentration to 50 mg mL^{-1}. The ratio between Ni^{2+} and total monomer concentration was 1:2000 in the process of yielding polymers with a molecular weight around 500 kg/mol, as determined by viscometry.

Synthesis of DBCO-Linkers. A DBCO-PEG4-SH (DBCO)-thiol linker for attachment to gold was synthesized as follows. Cysteammonium chloride ($HS(CH_2)_2NH_3Cl$) was dissolved in dimethylformamide at $c = 4$ mM. Next, 0.9 equiv DBCO−PEG4−NHS and 10 equiv diisopropylethylamine were added to the solution. The mixture was allowed to react on a rotating mixer for 24 h and was quenched with 10% TFA/DMSO to pH < 4. Finally, the product was diluted with purified (Milli-Q) water and further purified with HPLC.

Preparation of Thin PIC Films. The SPR sensor chips were prepared on BK7 glass substrates. Vacuum thermal evaporation (HHV AUTO 306 from HHV LTD.) was used for the deposition of the 2 nm layer of chromium, followed by a 50 nm layer of gold. The metal deposition rate was 2 Å s^{-1} in a vacuum better than 10^{-6} mbar. The gold surface of the prepared substrates was immersed in an ethanolic solution of 1 mM DBCO-thiol to form a self-assembled monolayer (SAM). After overnight incubation, the substrates were rinsed with copious amounts of ethanol to remove the excess of unbound

https://doi.org/10.1021/acs.jpcc.1c02489
J. Phys. Chem. C 2021, 125, 12960−12967

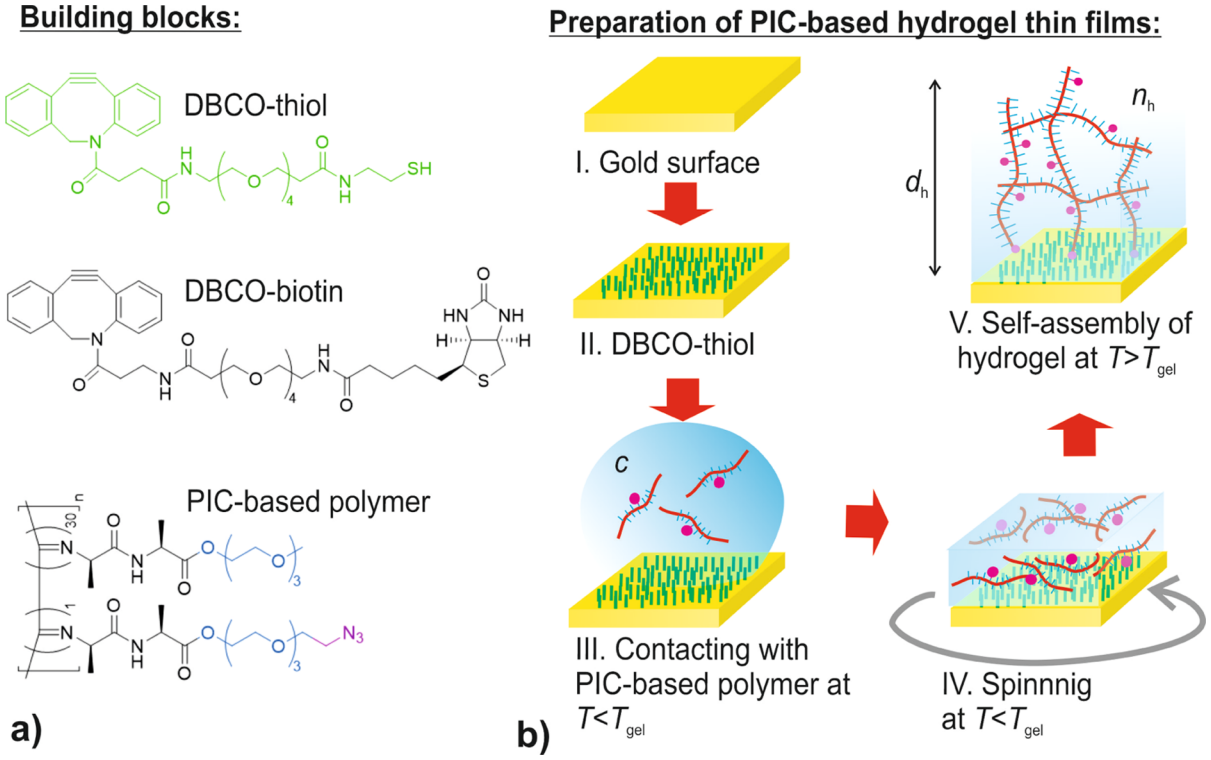

Figure 2. (a) Overview of used linkers and PIC-based copolymer and (b) preparation of thin PIC-based hydrogel films.

DBCO-thiol, dried in the stream of air, and placed on ice for at least 15 min. The 4 mg/mL stock solution of gelled PIC hydrogels was cooled below its gelation temperature T_{gel} (for the used copolymer of 15 °C). The obtained fluid polymer solution was diluted in cold ultrapure water to yield concentrations of c = 0.5, 1.0, 2.0, and 4.0 mg/mL. Then, 200 μL of each solution was pipetted on a separately cooled substrate with the DBCO-thiol SAM. The PIC solution on the top of such an SPR sensor chip was left on ice for 30 min to allow for click reaction between the azide groups carried out by the PIC chains and the DBCO moieties at the gold surface, which typically occurs in several minutes.[27] Afterward, the SPR sensor chip was spun at 1000 rpm for 30 s in order to yield a thin homogenous polymer film that was allowed to slowly reach room temperature. After 30 min, a dry surface of the PIC film was obtained and additional layers of the polymer were prepared by repeating the procedure with the spin rate lowered to 500 rpm.

Optical Setup. An in-house developed sensor instrument relying on angular interrogation of SPR and surface plasmon-enhanced fluorescence (SPFS) was used; see Figure 1. A monochromatic beam (λ_{ex} = 632.8 nm, 2 mW) was transverse magnetically (TM) or transverse electrically (TE) polarized by a polarizer (POL). The linearly polarized light beam passed through a chopper and was coupled to the 90° LASFN9 glass prism that was mounted on a rotation stage to control the angle of incidence θ. The SPR chip with a layer of an attached PIC-based hydrogel was optically matched to the prism base by using an immersion oil (Cargille Inc., USA). The intensity of the beam R that reflected at the SPR sensor chip surface was measured as a function of angle of incidence θ by a photodiode connected to a lock-in amplifier (EG&G, USA). Liquid samples were transported over the SPR sensor chip surface at a flow rate of 50 mL min^{-1} by using a flow cell connected to a Tygon tubing and a peristaltic pump (Ismatec, Germany). Fluorescence light emitted from the sensor surface in the perpendicular direction was collected through the flow cell made from a transparent glass substrate. It was excited by the evanescent field on the sensor surface at a wavelength λ_{ex}, and the emitted beam at wavelengths close to λ_{em} = 670 nm was collected by the lens. It was then spectrally cleaned by a notch filter (LNF, the central stop-band wavelength of 632.8 nm, XNF-632.8-25.0M, CVI Melles Griot, USA) and two bandpass filters (FBPF, transmission wavelength λ = 670 nm, 670FS10-25, Corporation Optical Filter, USA). The fluorescence intensity F was measured by a photomultiplier (H6240-01, Hamamatsu, Japan) that was connected to a counter (53131A, Agilent, USA). To minimize the bleaching of emitters, the intensity of the excitation laser beam at λ_{ex} was reduced to 1% by using a neutral-density filter (NDF, Linos Plano Optics). The angular reflectivity spectra $R(\theta)$ and fluorescence intensity $F(\theta)$ were recorded by a Wasplas software (Max Planck Institute for Polymer Research, Mainz, Germany).

Observation of Thin PIC-Based Hydrogel Layers. Thin layers of the PIC-based hydrogel were investigated in contact with air and water by using SPR combined with OWS. The thickness d_h and refractive index n_h of swollen hydrogel films and thickness $d_{h\text{-}dry}$ and refractive index $n_{h\text{-}dry}$ of dry hydrogel films were determined by fitting the reflectivity scans in TM and TE polarization $R(\theta)$ with a Fresnel reflectivity-based model implemented in WinSpall software (Max Planck Institute for Polymer Research, Germany). A "box" approximation was used, in which the layers were assumed to be homogeneous and a possible density gradient in the direction perpendicular to the surface was omitted. The swelling ratio SR of the PIC-based hydrogel layers was calculated from the experimentally found thickness of the hydrated and dry layers

https://doi.org/10.1021/acs.jpcc.1c02489
J. Phys. Chem. C 2021, 125, 12960−12967

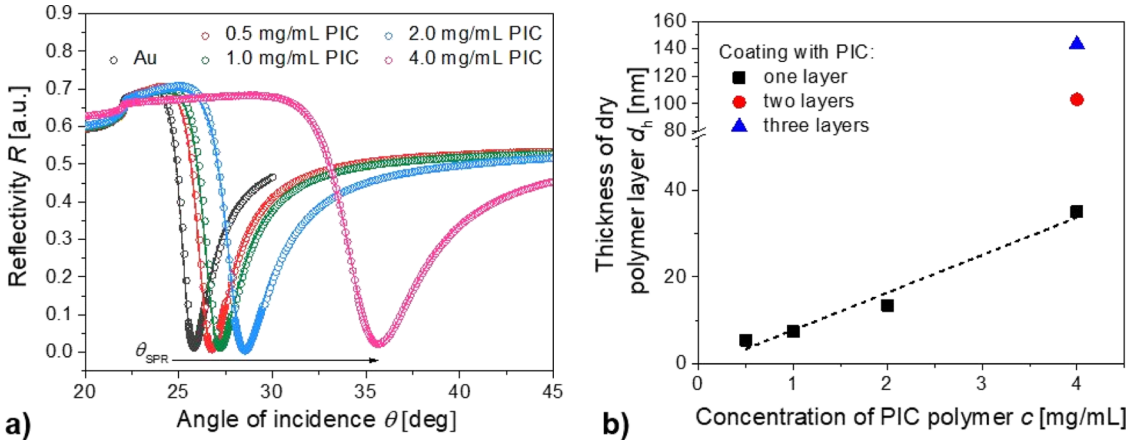

Figure 3. (a) Reflectivity spectra R for dry polymer films prepared from a solution of PIC polymer dissolved at concentration c = 0.5, 1, 2, and 4 mg/mL that was spun at 1000 rpm. (b) Measured dependence of the fitted thickness on c for one (1000 rpm), two (1000, 500 rpm), and three (1000, 500, 500 rpm) sequential depositions. The points were fitted with the linear function where $a = -0.93 \pm 2.3$ and $b = 8.66 \pm 1.0$.

$$\mathrm{SR} = \frac{d_h}{d_{h\text{-}dry}} \tag{1}$$

The respective polymer volume fraction f was obtained from the Maxwell Garnett effective medium theory as[17]

$$f = \frac{(n_h^2 - n_b^2)(n_{h\text{-}dry}^2 + 2n_b^2)}{(n_h^2 + 2n_b^2)(n_{h\text{-}dry}^2 - n_b^2)} \tag{2}$$

where n_b = 1.334 states the refractive index of buffer (PBS)[12] in contact with the polymer film, and n_h and $n_{h\text{-}dry}$ are the refractive indices of the hydrated and the dried PIC layers, respectively. The surface mass density Γ of the PIC-based hydrogel layer loaded with biomolecules was determined as[28]

$$\Gamma = (n_h - n_b) \times d_h \times \frac{\partial c}{\partial n} \tag{3}$$

where the coefficient $\partial n/\partial c$ = 0.2 μL/mg,[29] which describes the changes in the refractive index with the concentration of proteins.

Atomic Force Microscopy Analysis of PIC-Based Hydrogel Layers. The topography of dry PIC-based polymer layers was measured by using atomic force microscopy (PicoPlus from Molecular Imaging, Agilent Technologies, Germany) with tapping mode tips PPP-NCHR-50 (Nanosensors, Switzerland). The obtained images were processed in the open-source software Gwyddion (version 2.47 from gwyddion.net).

Post-Modification of PIC-Based Hydrogels. First, the SPR sensor chip carrying the PIC-based hydrogel layer was loaded onto the SPR sensor instrument (Figure 1). The surface was washed with PBS for 5 min, and then, 200 μM DBCO-biotin dissolved in PBS was reacted with the PIC hydrogel layer for 30 min. The excess of DBCO-biotin was removed by washing the sensor chip with PBS for 5 min. Subsequently, a solution of 200 μM NeutrAvidin was placed on top of the PIC hydrogel layer for 90 min, which was washed with PBS for 5 min. Then, biotinylated mouse IgG dissolved in PBS at a concentration of 50 μg/mL was allowed to bind to the PIC-based hydrogel matrix for 30 min. Finally, PBS with 2 μg/mL of rabbit anti-mouse IgG (that was tagged with the fluorescent dye Alexa Fluor-647) was flowed over the PIC-based hydrogel for 30 min, followed by rinsing with PBS for 5 min.

RESULTS AND DISCUSSION

Preparation of PIC-Based Hydrogel Layers. In order to graft the PIC hydrogel to the SPR sensor chip, its gold-coated surface was first reacted with a glycol linker carrying the thiol group and DBCO head group (DBCO-thiol); see Figure 2a. The DBCO-thiol was allowed to form a self-assembled monolayer[30] for the subsequent attachment of the PIC-based gel layer. As illustrated in Figure 2b, the PIC-based polymer was dissolved in water, which was cooled down below the gelation temperature T_{gel}, and the solution came in contact with the DBCO-modified gold surface. The PIC-based polymer in the solution reacted with the DBCO groups at the surface via its attached azide groups to establish a permanent graft. After the grafting reaction, the substrate with the polymer solution on its top was spun in order to form a thin hydrated layer. This layer was slowly heated to temperature T = 22 °C in 30 min, which is above the PIC polymer T_{gel}, and thus, the bundling of the polymer chains and respective gel formation can occur before it dries. The concentration of the PIC polymer in the aqueous solution was varied between 0.5 and 4 mg/mL to control the thickness and density of the PIC polymer-based film. The thickness of the dried film $d_{h\text{-}dry}$ was determined by SPR measurements from a shift of the SPR dip in the measured reflectivity spectrum $R(\theta)$, which was fitted with the Fresnel reflectivity-based model. As Figure 3a shows, SPR occurs at an angle of θ_{SP} = 25.8° on a bare gold surface (control without a PIC-based polymer layer). After the coating with the PIC layer, the SPR angle shifts to a higher angle (reaching up to θ_{SP} = 35.68° for the 4 mg/mL PIC solution). The analysis of measured spectra $R(\theta)$ allowed for determining the film thickness $d_{h\text{-}dry}$ in the range of 4−40 nm as presented in Figure 3b. It is worth noting that the film thickness $d_{h\text{-}dry}$ can be further increased by repeating the coating procedure. As it is shown in Figure 3b, repeated deposition of the PIC polymer from 4 mg/mL by using the same procedure with a decreased spin rate of 500 rpm yielded an increased thickness of $d_{h\text{-}dry}$ = 103 and 143 nm for two and three deposition cycles, respectively.

A previous study of the bulk PIC hydrogel structure showed that on average, seven helical polymer chains form a bundle with a diameter of 7.5 nm.[31] It was observed that the concentration of the polymer does not impact the bundle's diameter but rather their abundance and, as a result, the pore

https://doi.org/10.1021/acs.jpcc.1c02489
J. Phys. Chem. C 2021, 125, 12960−12967

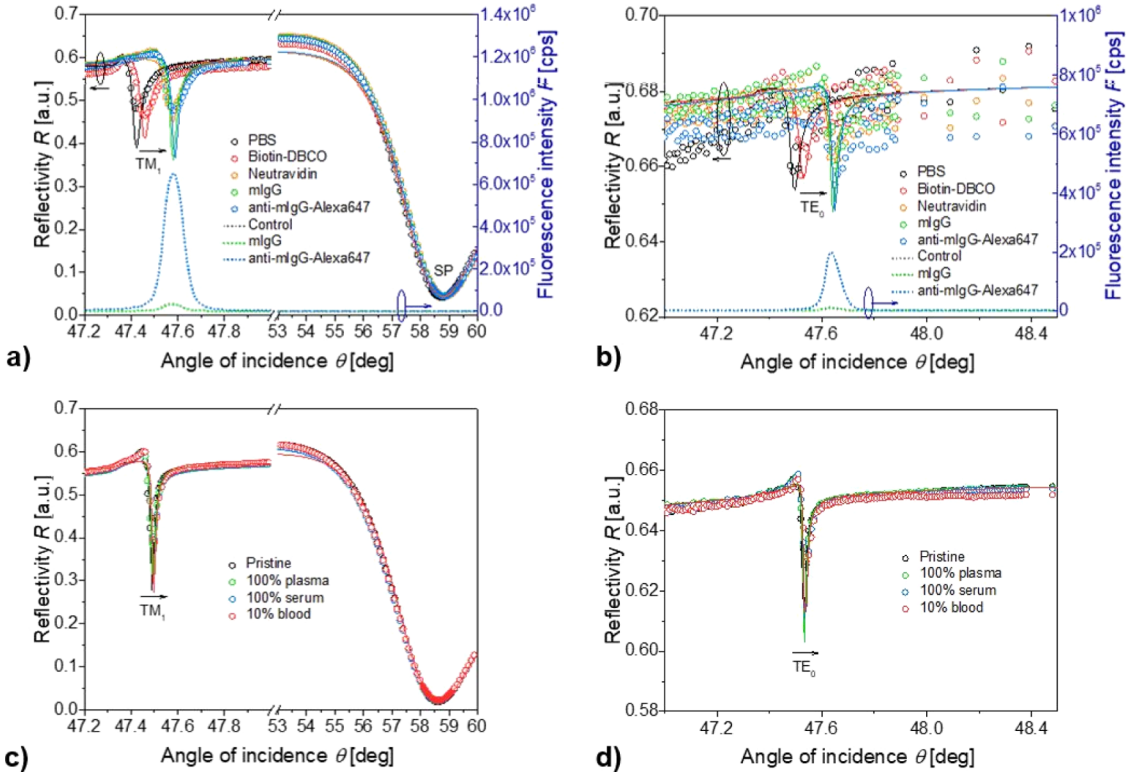

Figure 4. Changes in resonant coupling to (a) SP and TM_1 waves and (b) TE_0 wave upon a sequential reacting of the PIC hydrogel layer with biotin-DBCO, NeutrAvidin, mouse IgG, and anti-mouse IgG conjugated with Alexa Fluor 647 fluorophore. Changes in resonant coupling to (c) SP and TM_1 waves and (d) TE_0 wave upon after the exposure of PIC-based hydrogel to 10% blood, undiluted plasma, and undiluted serum.

size of the hydrogel matrix. Indeed, this observation was later confirmed by confocal fluorescence imaging, which showed a heterogeneous structure of interconnected fibrils with a pore size reaching 1−10 μm depending on the concentration.[32] The refractive index of the dry PIC polymer-based films prepared herein was determined as $n_{\text{h-dry}} = 1.4624$, which is below the value obtained for dense biopolymers and indicates that the structure comprises voids induced by the bundling of individual chains due to the formation of a network. The topography of the dry PIC polymer-based dry layer prepared from 4 mg/mL solution was characterized by using atomic force microscopy (see Figure S1). Our analysis of the thin polymer films revealed that the surface of the dry PIC-based polymer layer exhibits an rms roughness of ±4.2 nm, and we did not observe the fine structure of polymer bundles. The reason can be attributed to the fact that the bundles are rather densely packed in the investigated dry polymer layer.

Swelling of Thin PIC Hydrogel Layers. To prove that the grafted PIC polymer-based film forms a hydrogel, the layer was brought in contact with an aqueous liquid at room temperature (T = 22 °C, i.e., above the PIC gel temperature T_{gel}). Combined SPR and OWS were used for the SPR sensor chip carrying a PIC film with a dry thickness of $d_{\text{h-dry}} = 101$ nm and refractive index $n_{\text{h-dry}} = 1.4624$. The polymer layer came in contact with PBS, and angular reflectivity spectra $R(\theta)$ were measured for both TM and TE polarization, as shown in Figure 4a,b. Contrary to the measurement for a dry film (presented in Figure 3a), the angular spectra acquired from a film swollen in PBS show richer characteristics. The spectrum $R(\theta)$ exhibits two distinct resonances in TM polarization: besides the excitation of surface plasmons at $\theta_{\text{SP}} = 58.74°$, we observed an additional dielectric waveguide mode TM_1 at $\theta_{\text{TM}_1} = 47.42°$. Moreover, $R(\theta)$ in the orthogonal TE polarization shows a faint resonance at $\theta_{\text{TE}_0} = 47.50°$, which is associated with a dielectric waveguide mode TE_0. The analysis of the reflectivity spectra allowed us to determine the thickness d_{h} and the refractive index n_{h} of the hydrated PIC layer. It reveals that the thickness increased from $d_{\text{h-dry}} = 101$ nm to $d_{\text{h}} = 1558$ nm and refractive index decreased to $n_{\text{h}} = 1.3420$, close to that of water. These data indicate that the PIC polymer layer did not dissolve and that the formed polymer networks swelled by the uptake of water with the swelling ratio of SR = 15.4 determined from eq 1. These data imply a decreased polymer volume fraction f = 6.3%, based on eq 2, using the measured refractive indices n_{h}, $n_{\text{h-dry}}$, and that of PBS buffer $n_{\text{b}} = 1.334$. In addition, the respective surface mass density of the PIC-based hydrogel was calculated as $\Gamma = 62.3$ ng/mm^2 by using eq 3. This value is slightly lower than $\Gamma = 72.9$ ng/mm^2, which is determined for the dry film, prior to the swelling, due to the possible detachment of a small fraction of loosely bound polymer chains from the surface.

PIC-Based Hydrogel 3D Binding Matrix—Post-Modification. After establishing the protocol for the formation of a thin hydrogel layer on the gold substrate, we explored its application to serve as a three-dimensional binding matrix that can host biomolecules and allow for specific interactions with their affinity binding partners. In order to demonstrate this functionality, the azide groups on the PIC chains in the network were used for attaching functional biomolecules in a post-modification approach. The biofunctionalization steps were monitored by a combined SPR and OWS for a pristine hydrogel film with a thickness of $d_{\text{h}} = 1558$ nm and a refractive index of $n_{\text{h}} = 1.342$. This film exhibited a thickness of about 100 nm in the dry state, and it was prepared by two spin-

https://doi.org/10.1021/acs.jpcc.1c02489
J. Phys. Chem. C 2021, 125, 12960−12967

coating steps consisting of dispensing a solution with a polymer concentration of 4 mg/mL on the surface followed by its spinning at 1000 and 500 rpm (as represented in Figure 3b).

We utilized the well-known biotin−avidin interaction for the coupling of functional proteins to the PIC-based hydrogel.[33] In the first step, free azide moieties present on the PIC chains were reacted with the DBCO−biotin conjugate through the same catalyst-free click conjugation reaction that was used for substrate grafting (see Figure 2). After the reaction, the surface was rinsed with PBS, and we observed corresponding shifts in the resonant angles θ_{TM_1} and θ_{TE_0} in the reflectivity scans $R(\theta)$. The acquired shifts to $\theta_{TM_1} = 47.46°$ and $\theta_{TE_0} = 47.53°$ indicate that the surface mass density of the PIC-based hydrogel layer increased by 4.07 ng/mm^2 to $\Gamma = 66.40$ ng/mm^2 due to the attachment of biotin groups conjugated with DBCO (molecular weight 0.75 kDa). In the next step, the biotin groups on the PIC were allowed to bind to NeutrAvidin (molecular weight of 60 kDa). After rinsing away excess protein with PBS, the dielectric waveguide mode resonances shifted to values $\theta_{TM_1} = 47.58°$ and $\theta_{TE_0} = 47.65°$; these shifts correspond to a further increase of surface mass density by 15.57 ng/mm^2 to $\Gamma = 81.97$ ng/mm^2. It is worth noting that the measured surface mass density increase after the immobilization of NeutrAvidin is 4 times higher compared to that for the biotin−DBCO conjugate. However, the molecular weight ratio of these molecules of 80 is much larger, which indicates that only a limited fraction of available biotin groups reacted with the NeutrAvidin. A potential reason for this difference is that multiple biotin groups can bind one NeutrAvidin molecule (carrying four binding pockets). This avidity is associated with an additional cross-linking of the PIC hydrogel that may hinder the diffusion of molecules through the network and cause undesired crowding at the interface of the hydrogel film with the NeutrAvidin solution. In line with this observation, we noticed a negligible shift in the SPR angle θ_{SP} after the coupling of biotin with NeutrAvidin. The θ_{SP} angle probes about a 100 nm thin slice of the PIC-based hydrogel at its inner interface with the gold film. Therefore, the molecules reaching this interface need to diffuse through the whole PIC-based polymer network and may experience a more crowded environment due to the covalent attachment of the chains to the gold surface that thus hinders the affinity reaction.

PIC-Based Hydrogel as a 3D Binding Matrix—Immunoassay and Antifouling Properties. In order to demonstrate the functionality of the NeutrAvidin-modified PIC coating as a binding matrix for immunoassays, a biotinylated mouse IgG (mIgG) was affinity bound into the PIC film with NeutrAvidin molecules, followed by the binding of its affinity partner—a fluorophore-labeled anti-mIgG antibody. The first step was directly monitored by measuring a shift in the resonant angles θ_{TM_1} and θ_{TE_0}, as can be seen in Figure 4. The increase in surface mass density to $\Gamma = 82.45$ ng/mm^2 was determined by the analysis of these changes. Considering the IgG molecular weight of about 160 kDa, this surface mass density change indicates that only a small fraction of NeutrAvidin molecules inside the PIC-based hydrogel was available for reacting the mIgG−biotin molecules. A possible explanation for such decreased efficiency in the loading of this molecule to the PIC-based hydrogel layer is the crowding at the upper interface of the hydrogel occurring due to the densely packed NeutrAvidin and possibly, the additional cross-linking effect of reacting with mIgG carrying multiple biotin tags. The immobilized mIgG, however, was recognized by the anti-mIgG antibodies that were labeled with fluorophores Alexa Fluor 647 (A647), which allow for visualization by fluorescence spectroscopy. The fluorescence label was excited at $\lambda_{ex} = 633$ nm, coincident with the absorption band of A647 via the enhanced field intensity associated with the resonant excitation of the SP and dielectric waveguide modes TM_1 and TE_0. The binding of anti-mIgG conjugated with A647 gives rise to strong fluorescence peaks occurring in the angular scans $F(\theta)$ measured at the emission wavelength of $\lambda_{em} = 670$ nm at resonant angles θ_{TM_1} and θ_{TE_0}; see Figure 4a,b. These peaks show a strong intensity increase to $F = 6.5 \times 10^5$ cps for the TM_1 mode and 2×10^4 cps for the TE_0 mode, which corresponds to twenty times higher signal than the background indicating that, indeed, the PIC polymer gel can be used for sensing applications. Interestingly, no fluorescence signal increase was measured for θ_{SP}, which supports the hypothesis that the binding of IgG molecules primarily occurred at the interface of PIC hydrogel films for the used NeutrAvidin−biotin immobilization strategy.

It should be noted that for future applications, the properties of the hydrogel binding matrix should be optimized with respect to the size of the used ligand molecules and their affinity to the target analyte in order to enable their specific capture in the whole volume of the gel layer that is optically probed.[34] These steps would include adjusting the amount of coupled biotin groups (at the PIC polymer synthesis or by reacting the DBCO-biotin for a shorter time with the network), changing thickness d_h (by varying the PIC concentration in the solution and spinning rate), and adjusting pore size (by changing the PIC concentration). In addition, other coupling schemes that do not lead to the (unwanted) cross-linking may be beneficial to implement.

As sensing is often required in complex (biological) fluids, sensor fouling is a recurring problem. The resistance to fouling of the PIC hydrogel was tested using blood serum, plasma, and 10% diluted whole blood plasma. As seen in Figure 4c,d, a 15 min flow of these biological fluids followed by a 5 min rinse with PBS did not lead to a measurable shift in the resonances as measured for the surface plasmon modes SP or the dielectric waveguide modes TM_1 and TE_0 (Table S1 in Supporting Information). Overall, the 45 min exposure to various biological media resulted in the total shift of TM_1 and TE_0 modes by approximately 0.008° and an increase of surface mass density by less than $\Delta\Gamma = 1$ ng/mm^2. The antifouling nature of the PIC hydrogel can be assigned to the high level of hydration and presence of the relatively inert oligo(ethylene glycol) chains [as commonly used in self-assembled monolayers of alkanethiols with oligo(ethylene glycol) headgroups to prevent fouling of the sensor surfaces[35]]. Although the measurement of the resistance to nonspecific interactions of the PIC matrix shows its potential to serve as an efficient antifouling biointerface, the accuracy of the performed measurements does allow for comparison with the best performing antifouling materials known to date. For instance, the zwitterionic carboxybetaines and *N*-2-hydroxypropyl methacrylamide polymer brush layers were reported to prevent fouling of the complex media at a level of several pg/mm^2.[36] However, these biointerfaces exhibit a thickness that is about 2 orders of magnitude lower than the herein reported PIC-based

https://doi.org/10.1021/acs.jpcc.1c02489
J. Phys. Chem. C 2021, 125, 12960−12967

architecture, which consequently affects the surface mass density of deposited biomolecules.

CONCLUSIONS

In this paper, we deposited a PIC-based hydrogel on a solid surface in the form of a thin film and demonstrated that it can serve as an affinity binding matrix for sensing applications. The PIC gel is introduced on the chip in a two-step attachment procedure and the film thickness is readily controlled by the preparation conditions. The open fibrous structure of the hydrogel allows for diffusion of medium size protein molecules, which allows for post-modification of the polymer network with functional moieties. In our work, we demonstrated the functionalization with biotin and subsequent reaction with NeutrAvidin, which is a frequently used platform for further conjugation of biomolecules and implementation of assays including the immunoassay used herein. Hydrogel swelling and successive conjugation steps were monitored in a label-free manner by the combined SPR and OWS. Our work demonstrates that the PIC gels can be used to form stable hydrogel layers without the need for chemical or photo-cross-linking chemistry, which simplifies their preparation and is biomolecule-compatible. Also, the antifouling properties of the gel are advantageous. This study is the first step for the future development of robust PIC-based 3D sensor matrices for efficient affinity biosensors. The use of evanescent optical techniques may provide a facile tool for the characterization of such thin films in order to tailor them also for other application fields. For example, one can envision using a PIC-functionalized SPR sensor for simultaneous cell culturing and monitoring of cellular secretion molecules of interest.

ASSOCIATED CONTENT

Supporting Information

The Supporting Information is available free of charge at https://pubs.acs.org/doi/10.1021/acs.jpcc.1c02489.

> Calculation of the surface mass density of the hydrogel layers, AFM topography of a dry PIC-based polymer film prepared from 4 mg/mL solution and spun at 1000 rpm, and control experiment showing the changes in resonant coupling to (a) SP and TM_1 waves and (b) TE_0 wave upon reacting of neutravidin with the PIC hydrogel layer that was functionalized with biotin-DBCO (PDF)

AUTHOR INFORMATION

Corresponding Authors

Paul Kouwer − *Institute for Molecules and Materials, Radboud University, 6525 AJ Nijmegen, The Netherlands;* orcid.org/0000-0002-2760-191X; Phone: +31 024 3652464; Email: p.kouwer@science.ru.nl

Jakub Dostalek − *Biosensor Technologies, AIT-Austrian Institute of Technology GmbH, 3430 Tulln an der Dnau, Austria; FZU-Institute of Physics, Czech Academy of Sciences, Prague 182 21, Czech Republic;* orcid.org/0000-0002-0431-2170; Phone: +43 664 235 1773; Email: jakub.dostalek@ait.ac.at

Authors

Daria Kotlarek − *Biosensor Technologies, AIT-Austrian Institute of Technology GmbH, 3430 Tulln an der Dnau, Austria*

Kaizheng Liu − *Institute for Molecules and Materials, Radboud University, 6525 AJ Nijmegen, The Netherlands;* orcid.org/0000-0001-8555-4536

Nestor G. Quilis − *Biosensor Technologies, AIT-Austrian Institute of Technology GmbH, 3430 Tulln an der Dnau, Austria*

Dominik Bernhagen − *Pepscan Therapeutics, 8243 RC Lelystad, the Netherlands*

Peter Timmerman − *Pepscan Therapeutics, 8243 RC Lelystad, the Netherlands;* orcid.org/0000-0001-6687-5297

Complete contact information is available at: https://pubs.acs.org/10.1021/acs.jpcc.1c02489

Author Contributions

All authors have given approval to the final version of the manuscript.

Funding

D.K., K.L. and N.G.Q. received funding from the European Union's Horizon 2020 research and innovation programme under grant agreement no 642787, Marie Skłodowska-Curie Innovative Training Network BIOGEL. J.D. was supported by Lower Austria project IKTHEUAP number WST3-F-5030820/010-2019 and the ESIF and MEYS (FZU researchers, technical and administrative staff mobility−CZ.02.2.69/0.0/ 0.0/18_053/0016627).

Notes

The authors declare no competing financial interest.

ABBREVIATIONS

SPR, surface plasmon resonance; OWS, optical waveguide spectroscopy; PIC, polyisocyanide hydrogel; OEG, oligo(ethylene glycol) side chains; DBCO, dibenzocyclooctyne; SAM, self-assembled monolayer; TM, transverse magnetic; TE, transverse electric

REFERENCES

(1) Gibas, I.; Janik, H. Review : Synthetic Polymer Hydrogels for Biomedical. *Chem. Chem. Technol.* **2010**, *4*, 297.

(2) Zhang, X.-Z.; Wang, F. J.; Chu, C. C. Thermoresponsive Hydrogel with Rapid Response Dynamics. *J. Mater. Sci. Mater. Med.* **2003**, *14*, 451−455.

(3) Dai, S.; Ravi, P.; Tam, K. C. PH-Responsive Polymers: Synthesis, Properties and Applications. *Soft Matter* **2008**, *4*, 435−449.

(4) Zhao, Y.-L.; Stoddart, J. F. Azobenzene-Based Light-Responsive Hydrogel System. *Langmuir* **2009**, *25*, 8442−8446.

(5) Katsuno, C.; Konda, A.; Urayama, K.; Takigawa, T.; Kidowaki, M.; Ito, K. Pressure-Responsive Polymer Membranes of Slide-Ring Gels with Movable Cross-Links. *Adv. Mater.* **2013**, *25*, 4636−4640.

(6) Reddy, N. N.; Mohan, Y. M.; Varaprasad, K.; Ravindra, S.; Joy, P. A.; Raju, K. M. Magnetic and electric responsive hydrogel-magnetic nanocomposites for drug-delivery application. *J. Appl. Polym. Sci.* **2011**, *122*, 1364−1375.

(7) Culver, H. R.; Clegg, J. R.; Peppas, N. A. Analyte-Responsive Hydrogels: Intelligent Materials for Biosensing and Drug Delivery. *Acc. Chem. Res.* **2017**, *50*, 170−178.

(8) Cascone, S.; Lamberti, G. Hydrogel-Based Commercial Products for Biomedical Applications: A Review. *Int. J. Pharm.* **2020**, *573*, 118803.

(9) Homola, J.; Piliarik, M. Surface Plasmon Resonance (SPR) Sensors. In *Surface Plasmon Resonance Based Sensors*; Springer: Berlin, Heidelberg, 2006; pp 45−67.

(10) Löfås, S.; Johnsson, B. A Novel Hydrogel Matrix on Gold Surfaces in Surface Plasmon Resonance Sensors for Fast and Efficient

Covalent Immobilization of Ligands. *J. Chem. Soc., Chem. Commun.* **1990**, *21*, 1526−1528.
(11) Howell, S.; Kenmore, M.; Kirkland, M.; Badley, R. A. High-Density Immobilization of an Antibody Fragment to a Carboxymethylated Dextran-Linked Biosensor Surface. *J. Mol. Recognit.* **1998**, *11*, 200−203.
(12) Wang, Y.; Huang, C.-J.; Jonas, U.; Wei, T.; Dostalek, J.; Knoll, W. Biosensor Based on Hydrogel Optical Waveguide Spectroscopy. *Biosens. Bioelectron.* **2010**, *25*, 1663−1668.
(13) Huang, C.-J.; Jonas, U.; Dostálek, J.; Knoll, W. Biosensor Platform Based on Surface Plasmon-Enhanced Fluorescence Spectroscopy and Responsive Hydrogel Binding Matrix. *Opt. Sensors* **2009**, *2009*, 735625.
(14) Endo, T.; Ikeda, R.; Yanagida, Y.; Hatsuzawa, T. Stimuli-Responsive Hydrogel-Silver Nanoparticles Composite for Development of Localized Surface Plasmon Resonance-Based Optical Biosensor. *Anal. Chim. Acta* **2008**, *611*, 205−211.
(15) Toma, M.; Jonas, U.; Mateescu, A.; Knoll, W.; Dostalek, J. Active Control of SPR by Thermoresponsive Hydrogels for Biosensor Applications. *J. Phys. Chem. C* **2013**, *117*, 11705−11712.
(16) Sharma, N.; Keshmiri, H.; Zhou, X.; Wong, T. I.; Petri, C.; Jonas, U.; Liedberg, B.; Dostalek, J. Tunable Plasmonic Nanohole Arrays Actuated by a Thermoresponsive Hydrogel Cushion. *J. Phys. Chem. C* **2016**, *120*, 561−568.
(17) Zhang, Q.; Wang, Y.; Mateescu, A.; Sergelen, K.; Kibrom, A.; Jonas, U.; Wei, T.; Dostalek, J. Biosensor based on hydrogel optical waveguide spectroscopy for the detection of 17β-estradiol. *Talanta* **2013**, *104*, 149−154.
(18) Yang, W.; Xue, H.; Carr, L. R.; Wang, J.; Jiang, S. Zwitterionic Poly(Carboxybetaine) Hydrogels for Glucose Biosensors in Complex Media. *Biosens. Bioelectron.* **2011**, *26*, 2454−2459.
(19) Buzzacchera, I.; Vorobii, M.; Kostina, N. Y.; De Los Santos Pereira, A.; Riedel, T.; Bruns, M.; Ogieglo, W.; Möller, M.; Wilson, C. J.; Rodriguez-Emmenegger, C. Polymer Brush-Functionalized Chitosan Hydrogels as Antifouling Implant Coatings. *Biomacromolecules* **2017**, *18*, 1983−1992.
(20) Ahmed, E. M. Hydrogel: Preparation, Characterization, and Applications: A Review. *J. Adv. Res.* **2015**, *6*, 105−121.
(21) Kouwer, P. H. J.; de Almeida, P.; ven den Boomen, O.; Eksteen-Akeroyd, Z. H.; Hammink, R.; Jaspers, M.; Kragt, S.; Mabesoone, M. F. J.; Nolte, R. J. M.; Rowan, A. E.; et al. Controlling the Gelation Temperature of Biomimetic Polyisocyanides. *Chin. Chem. Lett.* **2018**, *29*, 281−284.
(22) Op 't Veld, R. C.; van den Boomen, O. I.; Lundvig, D. M. S.; Bronkhorst, E. M.; Kouwer, P. H. J.; Jansen, J. A.; Middelkoop, E.; Von den Hoff, J. W.; Rowan, A. E.; Wagener, F. A. D. T. G. Thermosensitive Biomimetic Polyisocyanopeptide Hydrogels May Facilitate Wound Repair. *Biomaterials* **2018**, *181*, 392−401.
(23) Das, R. K.; Gocheva, V.; Hammink, R.; Zouani, O. F.; Rowan, A. E. Stress-Stiffening-Mediated Stem-Cell Commitment Switch in Soft Responsive Hydrogels. *Nat. Mater.* **2016**, *15*, 318−325.
(24) Zimoch, J.; Padial, J. S.; Klar, A. S.; Vallmajo-Martin, Q.; Meuli, M.; Biedermann, T.; Wilson, C. J.; Rowan, A.; Reichmann, E. Polyisocyanopeptide Hydrogels: A Novel Thermo-Responsive Hydrogel Supporting Pre-Vascularization and the Development of Organotypic Structures. *Acta Biomater.* **2018**, *70*, 129−139.
(25) Weiden, J.; Voerman, D.; Dölen, Y.; Das, R. K.; Van Duffelen, A.; Hammink, R.; Eggermont, L. J.; Rowan, A. E.; Tel, J.; Figdor, C. G. Injectable Biomimetic Hydrogels as Tools for Efficient T Cell Expansion and Delivery. *Front. Immunol.* **2018**, *9*, 1−15.
(26) Liu, K.; Mihaila, S. M.; Rowan, A.; Oosterwijk, E.; Kouwer, P. H. J. Synthetic Extracellular Matrices with Nonlinear Elasticity Regulate Cellular Organization. *Biomacromolecules* **2019**, *20*, 826−834.
(27) Schoenmakers, D. C.; Rowan, A. E.; Kouwer, P. H. J. Crosslinking of Fibrous Hydrogels. *Nat. Commun.* **2018**, *9*, 1−8.
(28) Aulasevich, A.; Roskamp, R. F.; Jonas, U.; Menges, B.; Dostálek, J.; Knoll, W. Optical Waveguide Spectroscopy for the Investigation of Protein-Functionalized Hydrogel Films. *Macromol. Rapid Commun.* **2009**, *30*, 872−877.
(29) Perlmann, G. E.; Longsworth, L. G. The Specific Refractive Increment of Some Purified Proteins. *J. Am. Chem. Soc.* **1948**, *70*, 2719−2724.
(30) Vericat, C.; Vela, M. E.; Benitez, G.; Carro, P.; Salvarezza, R. C. Self-Assembled Monolayers of Thiols and Dithiols on Gold: New Challenges for a Well-Known System. *Chem. Soc. Rev.* **2010**, *39*, 1805−1834.
(31) Kouwer, P. H. J.; Koepf, M.; Le Sage, V. A. A.; Jaspers, M.; Van Buul, A. M.; Eksteen-Akeroyd, Z. H.; Woltinge, T.; Schwartz, E.; Kitto, H. J.; Hoogenboom, R.; et al. Responsive Biomimetic Networks from Polyisocyanopeptide Hydrogels. *Nature* **2013**, *493*, 651−655.
(32) Vandaele, J.; Louis, B.; Liu, K.; Camacho, R.; Kouwer, P. H. J.; Rocha, S. Structural characterization of fibrous synthetic hydrogels using fluorescence microscopy. *Soft Matter* **2020**, *16*, 4210−4219.
(33) Mandal, S.; Eksteen-Akeroyd, Z. H.; Jacobs, M. J.; Hammink, R.; Koepf, M.; Lambeck, A. J. A.; van Hest, J. C. M.; Wilson, C. J.; Blank, K.; Figdor, C. G.; et al. Therapeutic Nanoworms: Towards Novel Synthetic Dendritic Cells for Immunotherapy. *Chem. Sci.* **2013**, *4*, 4168−4174.
(34) Huang, C. J.; Dostalek, J.; Knoll, W. Long Range Surface Plasmon and Hydrogel Optical Waveguide Field-Enhanced Fluorescence Biosensor with 3D Hydrogel Binding Matrix: On the Role of Diffusion Mass Transfer. *Biosens. Bioelectron.* **2010**, *26*, 1425−1431.
(35) Zhu, B.; Eurell, T.; Gunawan, R.; Leckband, D. Chain-length dependence of the protein and cell resistance of oligo(ethylene glycol)-terminated self-assembled monolayers on gold. *J. Biomed. Mater. Res.* **2001**, *56*, 406−416.
(36) Rodriguez-Emmenegger, C.; Houska, M.; Alles, A. B.; Brynda, E. Surfaces Resistant to Fouling from Biological Fluids: Towards Bioactive Surfaces for Real Applications. *Macromol. Biosci.* **2012**, *12*, 1413−1422.

https://doi.org/10.1021/acs.jpcc.1c02489
J. Phys. Chem. C 2021, 125, 12960−12967